A circadian-regulated gene, *Nocturnin*, promotes adipogenesis by stimulating PPAR-γ nuclear translocation

Masanobu Kawai[a], Carla B. Green[b,1], Beata Lecka-Czernik[c], Nicholas Douris[b], Misty R. Gilbert[b], Shihoko Kojima[b,1], Cheryl Ackert-Bicknell[d], Neha Garg[e], Mark C. Horowitz[f], Martin L. Adamo[e], David R. Clemmons[g], and Clifford J. Rosen[a,2]

[a]The Musculoskeletal Laboratory, Maine Medical Center Research Institute, Scarborough, ME 04074; [b]Department of Biology, University of Virginia, Charlottesville, VA 22904; [c]Department of Orthopaedic Surgery, Center for Diabetes and Endocrine Research, University of Toledo Medical Center, Toledo, OH 43614; [d]The Jackson Laboratory, Bar Harbor, ME 04609; [e]Department of Biochemistry, University of Texas Health Science Center at San Antonio, San Antonio, TX 78229; [f]Department of Orthopaedics and Rehabilitation, Yale University School of Medicine, New Haven, CT 06520; and [g]Department of Medicine, University of North Carolina, School of Medicine, Chapel Hill, NC 27599

Nocturnin (NOC) is a circadian-regulated protein related to the yeast family of transcription factors involved in the cellular response to nutrient status. In mammals, NOC functions as a deadenylase but lacks a transcriptional activation domain. It is highly expressed in bone-marrow stromal cells (BMSCs), hepatocytes, and adipocytes. In BMSCs exposed to the PPAR-γ (peroxisome proliferator-activated receptor-γ) agonist rosiglitazone, *Noc* expression was enhanced 30-fold. Previously, we reported that $Noc^{-/-}$ mice had low body temperature, were protected from diet-induced obesity, and most importantly exhibited absence of *Pparg* circadian rhythmicity on a high-fat diet. Consistent with its role in influencing BMSCs allocation, $Noc^{-/-}$ mice have reduced bone marrow adiposity and high bone mass. In that same vein, NOC overexpression enhances adipogenesis in 3T3-L1 cells but negatively regulates osteogenesis in MC3T3-E1 cells. NOC and a mutated form, which lacks deadenylase activity, bind to PPAR-γ and markedly enhance PPAR-γ transcriptional activity. Both WT and mutant NOC facilitate nuclear translocation of PPAR-γ. Importantly, NOC-mediated nuclear translocation of PPAR-γ is blocked by a short peptide fragment of NOC that inhibits its physical interaction with PPAR-γ. The inhibitory effect of this NOC-peptide was partially reversed by rosiglitazone, suggesting that effect of NOC on PPAR-γ nuclear translocation may be independent of ligand-mediated PPAR-γ activation. In sum, *Noc* plays a unique role in the regulation of mesenchymal stem-cell lineage allocation by modulating PPAR-γ activity through nuclear translocation. These data illustrate a unique mechanism whereby a nutrient-responsive gene influences BMSCs differentiation, adipogenesis, and ultimately body composition.

Several lines of evidence demonstrate a relationship between circadian networks and adipogenesis. For example, alterations in time-keeping among individuals on psychotropic drugs, nighttime shift workers, or those with hormonal imbalances are often associated with fat redistribution (1–3). The nuclear receptor and transcription factor PPAR (peroxisome proliferator-activated receptor)-γ2 and PGC-1α (PPAR-γ coactivator 1-α) both exhibit cell-autonomous circadian patterns of gene expression (4). PPAR-γ2 is also critical in mesenchymal cell specification (5), a process under the influence of circadian networks. Activation of PPAR-γ2 with aging or by the PPAR-γ agonist rosiglitazone is negatively correlated with osteogenesis and positively with bone marrow adipogenesis, although *Pparg* haploinsufficiency in mice results in high bone mass, leanness, and little marrow fat (5, 6).

Mammalian time-keeping is regulated by hypothalamic and peripheral clock genes (7–11). *Nocturnin* (*Noc*; *Ccrn4l*) is one of several cell-autonomous circadian genes (12) whose expression is high in liver, hypothalamus, and adipocytes, and whose production peaks in early night (13). *Noc* encodes a deadenylase that removes poly-A tails from the 3′ ends of mRNAs (14, 15).

Previously, we reported that *Noc* gene expression was up-regulated nearly 30-fold in bone-marrow stromal cells (BMSCs) transfected with *Pparg2* and exposed to rosiglitazone (16). Similarly, in a congenic mouse with low bone mass and increased *Pparg* activity, *Noc* transcripts were markedly enhanced in liver, fat, and bone marrow (17). In hepatic and skeletal tissues from aging rodents, there is increased *Noc* expression coincident with greater PPAR-γ2 activity, low bone mass, and greater bone-marrow adiposity (18). In addition, we have also shown that $Noc^{-/-}$ mice are protected from diet-induced obesity and exhibited absence of circadian *Pparg* expression, even on a high-fat diet (19). These data led us to hypothesize there is an important interaction between NOC and PPAR-γ that facilitates adipogenesis. Here, we present the molecular mechanism underlying this interaction in which NOC stimulates PPAR-γ function by facilitating its nuclear localization. These observations suggest that *Noc* modulates BMSCs fate by shifting stem cells into the adipogenic lineage and away from osteoblast differentiation. More importantly, these lines of evidence reinforce the importance of circadian networks in the regulation of body composition.

Results

Noc Stimulates Adipogenesis and Suppresses Osteoblastogenesis. First, to understand the role of *Noc* during mesenchymal stromal cell differentiation, the critical first step in osteoblast and adipocyte differentiation, we examined the temporal profile of *Noc* expression. We found *Noc* was up-regulated during adipogenesis in both 3T3-L1 and OP9 cells (Fig. 1 *A* and *B* and Fig S1). Surprisingly, *Noc* expression was induced coincident with PPAR-γ1 in early adipogenesis and before PPAR-γ2 (Fig. 1B). Overexpression of *Noc* in 3T3-L1 cells markedly stimulated adipogenesis and was accompanied by a significant increase in *aP2* (fatty acid-binding protein 4) and *Pparg2* expression (Fig. 1 *C* and *D* and Fig S2). Consistently, knockdown of *Noc* in 3T3-L1 cells suppressed adipogenesis and was associated with reduced expression of adipogenic markers including *Pparg2*, *aP2*, and *Lpl* (lipoprotein lipase) (Fig. 1 *E* and *F* and Fig S2). In contrast, *Noc* expression was down-regulated during osteoblastogenesis of primary calvarial osteoblasts (COBs) (Fig. 1 *G* and *H*), and

Fig. 1. NOC favors adipogenesis over osteoblastogenesis. (A and B) 3T3-L1 cells were treated with control media (cont or C) or adipogenic mixture (Adipo or A) for 9 d. Expression of aP2 and Noc was analyzed by real-time PCR (n = 3) (A), and protein levels of PPAR-γ and Noc were determined by Western blot analysis at indicated time points (B). (C and D) GFP or Noc overexpressing 3T3-L1 cells were treated with adipogenic mixture. At day 7, Oil-red O staining (C) and real-time PCR for aP2 and Pparg2 (D) were performed (n = 3). (E) 3T3-L1 cells stably expressing either control or Noc-shRNA were treated with adipogenic media, and Oil-red O staining was performed at day 7. (F) Noc expression was suppressed using siRNA in 3T3-L1 cells. At indicated time points after adipogenic induction, expression of marker genes for adipogenesis was analyzed by real-time PCR (n = 3). Expression of Noc, Pparg2, aP2, and C/EBPα was normalized to 36B4 and expression of LPL and RXRα was normalized to β2-microglobulin. (G and H) Primary COBs from Noc+/+ and Noc−/− mice were treated with control (con) or osteogenic (OB) media for 11 d. Noc expression during osteoblastogenesis was analyzed in Noc+/+ cells using real-time PCR (n = 4) (G) and Western blot analysis (H). (I and J) GFP or Noc overexpressing MC3T3-E1 cells were treated with osteogenic media. At days 7 and 28, alkaline phosphatase (ALP) and Von Kossa staining (I), and real-time PCR for ALP, and OC were performed (n = 3) (J). (K and L) MC3T3-E1 cells stably expressing either control or Noc-shRNA were treated with osteogenic media. ALP and Von Kossa staining (K) were performed at day 7 and 28, and expression of ALP and OC were examined by real-time PCR at day 28 (n = 3) (L). (M and N) Primary COBs from Noc+/+ and Noc−/− mice were treated with osteogenic media, and ALP and Von Kossa staining (M), and real-time PCR for Runx2, ALP, and OC were performed at day 11 (n = 5) (N). Figures shown are the representative of at least three independent experiments. Values are expressed as the mean ± SEM. †, P < 0.001; *, P < 0.01; **, P < 0.05.

COBs derived from Noc−/− mice had lower Pparg and higher Runx2 expression compared with controls (Fig S3A). Overexpression of Noc in MC3T3-E1 cells suppressed osteoblastogenesis with reduced expression of *alkaline phosphatase* (ALP) and *Osteocalcin* (OC) (Fig. 1 I and J and Fig S2), whereas knockdown of Noc in MC3T3-E1 cells stimulated osteoblastogenesis with increased expression of *ALP* and *OC* (Fig. 1 K and L and Fig S2). Consistent with this, Noc −/− COBs, when exposed to osteogenic media, also showed enhanced osteogenesis compared with control cells (Fig. 1 M and N). The findings that NOC enhances *Pparg2* expression and decreases *Runx2* expression led us to hypothesize that NOC affects the transcription of these genes. To test this tenet, we performed reporter assays using luciferase vectors fused with either the *Runx2* promoter (0.6 kb) or the *Pparg2* promoter (0.9 kb). To investigate whether the

deadenylase activity of NOC is involved in this regulation, we also used a magnesium-binding motif mutant of NOC (E193A-Noc), which lacked deadenylase activity. However, neither WT nor mutant NOC affected the luciferase activity of these constructs (Fig S3B). The increase in *Runx2* expression in Noc−/− COBs was not accompanied by a craniofacial phenotype, which was assessed at postnatal day 7 by inspection with microCT (Fig S3C). Notwithstanding, because the promoter size inserted in these luciferase vectors is small, we cannot exclude the possibility that the regulatory region may exist outside of tested promoter fragments. In sum, *Noc* modulates BMSCs' fate by shifting cells into the adipogenic pathway and away from the osteoblast lineage.

NOC Is Physically and Functionally Associated with PPAR-γ Independent of Its Deadenylase Activity. Based on the temporal profile of *Noc* expression in adipocytes, we next sought to determine whether *Noc* influenced adipogenesis by regulating PPAR-γ. As described previously, NOC had no effect on the activity of the luciferase vector containing *Pparg2* promoter, but interestingly, we found that NOC coimmunoprecipitated with both PPAR-γ1 and PPAR-γ2, demonstrating a physical interaction between these proteins (Fig. 2A and Fig S4A). Based on the exclusive expression and the critical role of *Pparg2* in adipocytes, we analyzed the interaction between *Pparg2* and *Noc* in this study. In a reporter assay using a luciferase vector containing a *Pparg* response element, WT Noc did not affect the basal *Pparg2* transcriptional activity, but *Pparg2* transcriptional activation by rosiglitazone was significantly increased in the presence of WT Noc in murine marrow-derived UAMS-33 cells stably expressing *Pparg2* expression vector (U-33/γ2 cells) (Fig. 2B). Consistently,
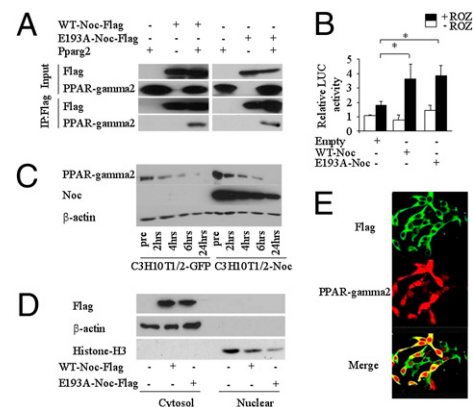
Fig. 2. NOC is physically and functionally associated with PPAR-γ2 in a deadenylase-independent manner. (A) HEK293 cells were transfected with WT-Noc-Flag or E193A-Noc-Flag, or a Pparg2-expression vector. Immunoprecipitation with Flag was followed by Western blot analysis for PPAR-γ. (B) Reporter assay using Pparg response element (PPRE) containing luciferase vector in the presence or absence of 1 μM rosiglitazone (n = 3) was performed using murine marrow-derived UAMS-33 cells stably expressing Pparg2-expression vector (U-33/γ2 cells). (C) C3H10T1/2 cells overexpressing Noc or GFP were transfected with Pparg2-expression vector, and treated with 10 μg/mL cycloheximide. Whole-cell lysate was collected at indicated time points, and expression of PPAR-γ, Noc, and β-actin was examined by Western blot analysis. (D) HEK293 cells were transfected with WT-Noc-Flag or E193A-Noc-Flag expression vector, and cell fractionation was performed. Noc expression was analyzed by Western blot analysis with anti-Flag antibody. β-actin and Histone-H3 were examined as a positive control for cytosol and nuclear protein, respectively. (E) HEK293 cells were cotransfected with WT-Noc-Flag and a Pparg2-expression vector and treated with 5 μM of rosiglitazone. Noc and Pparg expression were visualized by immunofluorescence using anti-Flag antibody and anti-PPAR-γ antibody. Figures shown are the representative of at least three independent experiments. Values are expressed as the mean ± SEM. *, P < 0.05.

CELL BIOLOGY
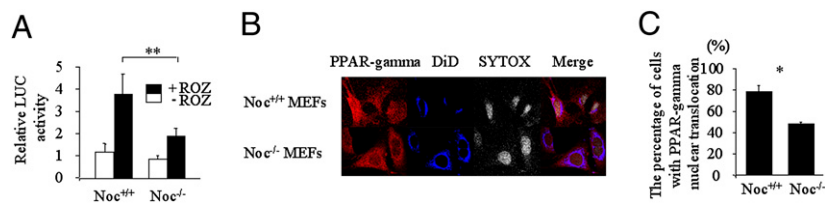
Fig. 3. Lack of Noc in MEFs decreases PPAR-γ transcriptional activation by rosiglitazone and PPAR-γ nuclear expression. (*A*) Mouse MEFs from WT or *Noc⁻/⁻* mice were transfected with Pparg2 expression vector and PPRE containing luciferase vector. Twenty-four hours after transfection, cells were treated with 1 μM rosiglitazone for 24 h and reporter assay was performed (*n* = 4–5). (*B* and *C*) Immunofluorescence using conforcal microscopy was performed to detect PPAR-γ expression in WT or *Noc⁻/⁻* MEFs (*B*) and the percentage of cells exhibiting PPAR-γ nuclear expression was quantitated by immunofluorescence. At lease 20 cell were counted for quantification (*n* = 4) (*C*). Figures shown are the representative of at least three independent experiments. Values are expressed as the mean ± SEM. *, *P* < 0.01; **, *P* < 0.05.

Pparg2 transcriptional activation by rosiglitazone was impaired in *Noc*-deficient mouse embryonic fibroblasts (MEFs) compared with WT MEFs, although basal transcriptional activity was comparable between WT and *Noc⁻/⁻* MEFs (Fig. 3*A*). To examine whether physical binding of NOC to PPAR-γ2 caused any alteration in the stability of PPAR-γ2, C3H10T1/2 cells over-expressing either GFP or *Noc* were transfected with a *Pparg2* expression vector and treated with cyclohexamide to inhibit protein synthesis. Western blot analysis for PPAR-γ2 revealed that, although PPAR-γ2 levels before cyclohexamide treatment were increased in cells overexpressing *Noc*, *Noc* did not influence the PPAR-γ2 degradation rate (Fig. 2*C*).

Next, we investigated whether the physical association between NOC and PPAR-γ2 was part of the deadenylation process. For this purpose, we used a mutant of NOC (E193A-Noc) that lacked deadenylase activity. Coimmunoprecipitation analysis revealed that E193A-Noc bound to PPAR-γ2 in a manner identical to the WT Noc (Fig. 2*A*). U-33/γ2 cells expressing E193A-Noc also showed a significant increase in PPAR-γ2 transcriptional activation by rosiglitazone (Fig. 2*B*). To test whether NOC functions as a transcriptional coactivator for PPAR-γ2, we analyzed the intracellular localization of WT NOC and E193A-NOC. Immunofluorescence and Western blotting analyses confirmed that NOC was present exclusively in the cytoplasm even in the presence of PPAR-γ2 activation (Fig. 2 *D* and *E*), thereby ruling out the possibility that NOC acts as a transcriptional coactivator of PPAR-γ. Taken together, these data demonstrate that NOC binds to PPAR-γ2 and activates PPAR-γ2 transcriptional activity in a deadenylase-independent manner.

NOC Stimulates PPAR-γ Nuclear Translocation. To clarify the role of NOC in PPAR-γ2 activation, we performed immunofluorescence and found that NOC exhibited perinuclear localization (Fig. 4*A*). This finding led us to hypothesize that NOC assisted PPAR-γ2 translocation into the nucleus in part by retaining it at the nuclear membrane. To answer this question, we examined intracellular localization of PPAR-γ2 using HEK293 cells transfected with *Pparg2* and *Noc*. In HEK293 cells PPAR-γ2 mainly resided in the cytoplasm. However, with overexpression of *Noc,* PPAR-γ2 translocated into the nucleus even in the absence of a PPAR-γ2 agonist (Fig. 4 *B* and *C*). We also analyzed the nuclear translocation of PPAR-γ1, and found the same effect of NOC on PPAR-γ1 nuclear translocation (Fig S4*B*). Consistent with these data, the percentage of cells exhibiting nuclear PPAR-γ expression was reduced in *Noc⁻/⁻* MEFs compared with WT cells (Fig. 3 *B* and *C*). E193A-Noc, the mutated NOC without deadenylase activity, also facilitated PPAR-γ2 nuclear translocation (Fig. 4 *B* and *C*), demonstrating that NOC facilitates PPAR-γ2 nuclear translocation in a deadenylase-independent manner. In addition, cells expressing N-terminal truncation of NOC (S64-F429 NOC), which lacks the first 63 amino acids, also showed enhancement of PPAR-γ2 nuclear transport (Fig S4*C*).

Finally, to determine the binding site of NOC to PPAR-γ, we studied the full-length NOC protein and identified a region (amino acids 341–351) with sequence similarity to an Src homology 2 domain binding motif. We then generated a short peptide that corresponded to amino acids 341 to 351 in NOC and fused it to a TAT protein (20) in its N terminus (NOC-peptide) to test whether this sequence could prevent the NOC/PPAR-γ interaction. Addition of NOC-peptide (1 μM) inhibited the binding of NOC to PPAR-γ2 (Fig. 5*A*) and significantly blocked NOC-stimulated endogenous PPAR-γ nuclear translocation in 3T3-L1 cells expressing WT-NOC (Fig. 5 *B* and *C*). In addition, NOC-peptide inhibited endogenous PPAR-γ transcriptional activity in 3T3-L1 cells (Fig. 5*D*).

Next, we investigated whether nuclear translocation of PPAR-γ by NOC is affected by ligand activation with rosiglitazone and if rosiglitazone could antagonize the effect of NOC-peptide. Rosi-
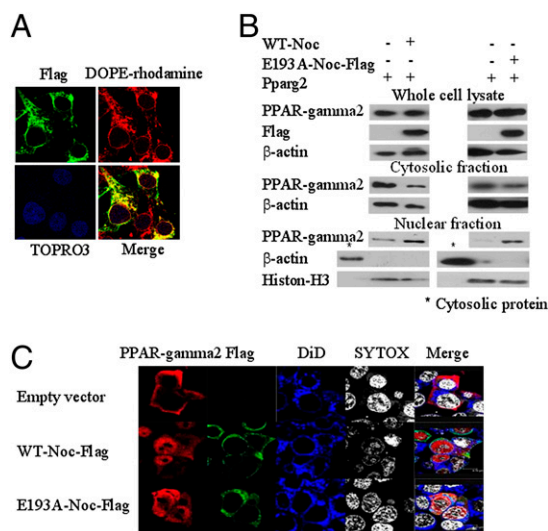
Fig. 4. NOC shows perinuclear localization, and enhances nuclear transport of PPAR-γ2 in a deadenylase-independent manner. (*A*) HEK293 cells were transfected with WT-Noc-Flag expression vector. Noc expression was visualized by immunofluoresence using anti-Flag antibody. DOPE-rhodamine was used to detect nuclear membrane, and TOPRO3 was used for nuclear staining. (*B* and *C*) HEK293 cells were tranfected with either WT-Noc-Flag or E193A-Noc-Flag, or a Pparg2 expression vector. Immunofluorescence using conforcal microscopy was performed to detect PPAR-γ expression (*B*). Cell fractionation was performed, and Western blot analysis for PPAR-γ was carried out. β-actin and Histone-H3 were examined as a positive control for cytosol and nuclear protein, respectively. The cytosolic fraction from HEK293 cells was used as a positive control for β-actin and a negative control for Histone-H3 (*Left* lane in nuclear fraction) (*C*). Figures shown represent at least three independent experiments.
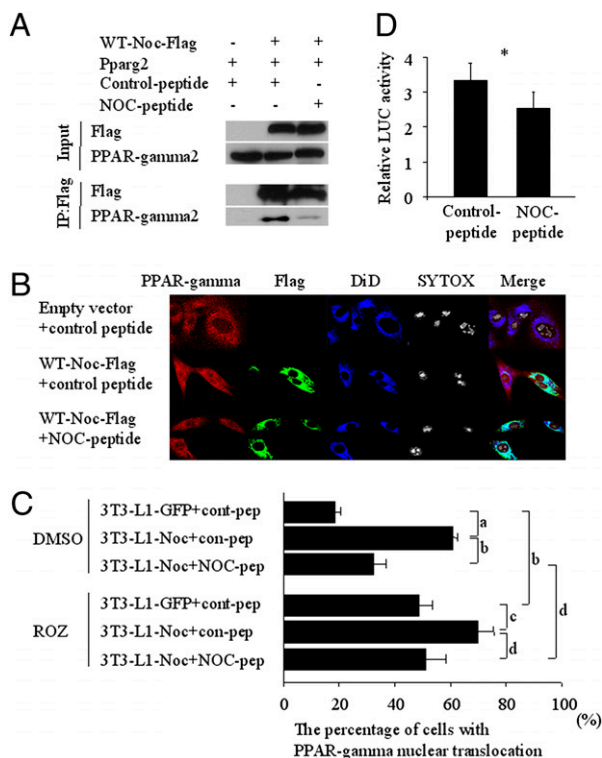
Fig. 5. Amino acid 341–351 in the NOC protein is responsible for the binding between NOC and PPAR-γ2. (A) HEK293 cells were tranfected with a Pparg2 or WT-Noc-Flag expression vector in the presence of 5 μg/mL NOC-peptide or control peptide, and immunoprecipitation with Flag was followed by Western blot analysis for PPAR-γ (n = 4). (B) 3T3-L1 cells overexpressing GFP or WT-Noc-Flag were incubated with NOC-peptide or control peptide, and the expression of PPAR-γ and Noc was visualized by immunofluorescence. (C) 3T3-L1 cells overexpressing GFP or WT-Noc-Flag were incubated with NOC-peptide or control peptide in the presence of DMSO or 1 μM of rosiglitazone (ROZ) and the percentage of cells exhibiting PPAR-γ nuclear translocation was quantitated by immunofluorescence. At lease 20 cell were counted for quantification (n = 5). (D) 3T3-L1 cells were transfected with PPRE-Luc construct in the presence of 5 μg/mL NOC-peptide or control peptide, and luciferase assay was performed at day 2 (n = 4). Figures shown represent at least four independent experiments. Values are expressed as the mean ± SEM. *, P < 0.05; a, P < 0.0001; b, P < 0.001; c, P < 0.01; d, P < 0.05.

glitazone induced nuclear translocation of PPAR-γ in 3T3-L1 cells expressing GFP (3T3-L1-GFP cells) treated with control peptide, and treatment with rosiglitazone in 3T3-L1 cells expressing Noc (3T3-L1-Noc cells) further increased nuclear translocation of PPAR-γ compared with 3T3-L1-Noc cells, although this did not reach statistical significance (Fig. 5C). In addition, rosiglitazone partially but significantly blocked the inhibitory effect of NOC-peptide on PPAR-γ nuclear translocation. These lines of evidence suggest that the effect of NOC on PPAR-γ nuclear translocation is in part mediated by the mechanism independent of rosiglitazone-induced PPAR-γ nuclear translocation (Fig. 5C). In sum, NOC mediates nuclear activation of PPAR-γ by facilitating nuclear transport through binding to the region corresponding to amino acid 341 to 351 in the NOC protein.

Body Composition Phenotype of Noc$^{-/-}$ Mice. Previously, we reported that Noc$^{-/-}$ mice were protected from high-fat diet (HFD)-induced obesity (19). Generally, Pparg exhibits a circadian rhythm in liver that is amplified by a HFD (4, 19). However, Pparg circadian gene expression was absent on a HFD in Noc$^{-/-}$ mice, suggesting Pparg function could be altered in Noc$^{-/-}$ mice (19). Thus, we further characterized the adipogenic and skeletal
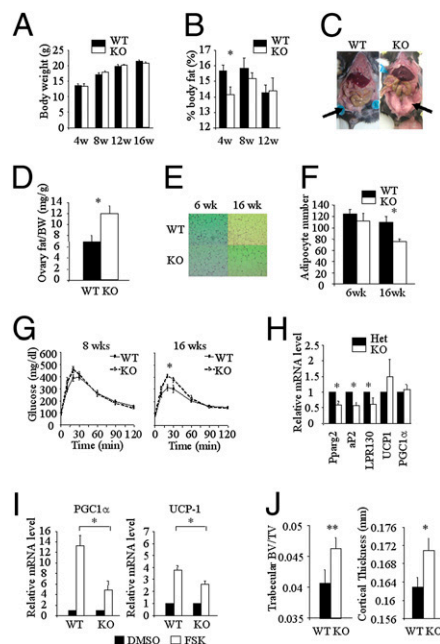
Fig. 6. Body composition and fat characteristics of Noc$^{-/-}$ mice. (A and B) Body weight (A) and percent body fat (B) was measured in Noc$^{+/+}$ (n = 13–16) and Noc$^{-/-}$ (n = 10) mice at the ages indicated. (C and D) The gross appearance of the ovarian fat pad (arrow in C) and ovarian fat pad weight (D) was examined in 16-wk-old Noc$^{+/+}$ (n = 8) and Noc$^{-/-}$ (n = 5) mice. (E and F) The ovarian fat pad from 6- and 16-wk-old mice was examined histologically by H&E staining (E), and the number of adipocytes per field was determined (n = 4) (F). (G) Glucose tolerance was determined at 8 (n = 9–13) and 16 wk of age (n = 7). (H and I) Primary brown preadipocytes from 10-d-old mice were differentiated to brown adipocytes and the expression of brown adipocyte-related genes was examined by real-time PCR (n = 4–5) (H). Primary brown adipocytes were treated with forskolin (10 μM) for 4 h and expression of PGC1α and UCP-1 was analyzed by real-time PCR (n = 3) (I). (J) Trabecular BV/TV in distal femur was measured by microCT (Left, n = 25–26), and cortical thickness at the midshaft of femur was assessed by peripheral quantitative CT (Right, n = 21) at 16 wk of age. Values are expressed as the mean ± SEM. *, P < 0.05; **, P < 0.01.

phenotype of Noc$^{-/-}$ mice to clarify the in vivo consequence of the lack of Noc. We found that total body weight did not differ from controls across several time points (Fig. 6A), although percent body fat was less than controls at 4 wk of age (Fig. 6B). At 16 wk, Noc$^{-/-}$ mice accumulated more ovarian fat accompanied by hypertrophic adipocytes (Fig. 6 C–F). In addition, Noc$^{-/-}$ mice developed moderate glucose intolerance (Fig. 6G). In the bone marrow of Noc$^{-/-}$ mice there were fewer adipocytes compared with controls (Fig S5). The size of brown adipose tissue (BAT) was not different among the three genotypes of Noc, but BAT from Noc$^{-/-}$ mice showed an increase in accumulation of lipid droplets compared with Noc$^{+/+}$ or Noc$^{+/-}$ mice (Fig S6 A and B). There was no difference in brown adipogenesis of the stromal vascular fraction from BAT among the three genotypes (Fig S6C). Furthermore, BAT-related gene expression was not different between Noc$^{+/+}$ and Noc$^{+/-}$ brown adipocytes (Fig S6D), but expression of Pparg2, aP2, and LRP130 (leucine-rich PPR motif-containing protein; LRPPRC), which is downstream of PGC-1α and modulates brown adipocyte function (21), were significantly decreased in Noc$^{-/-}$ brown adipocytes (Fig. 6H). Basal expression of UCP-1 (uncoupling protein 1) and PGC1α did not differ by genotype (Fig. 6H and Fig S6D), but induction of UCP-1 and PGC1α by forskolin was significantly impaired in the Noc$^{-/-}$ cells vs. control cells (Fig. 6I). In sum, Noc$^{-/-}$ mice have impaired ex vivo BAT function, which would be consistent with the lower basal body temperature reported previously (19).

In respect to skeletal composition, $Noc^{-/-}$ mice exhibited higher areal whole-body and femoral bone mineral density (aBMD) than controls (Table S1). Femoral areal bone mineral content (aBMC) was significantly higher in $Noc^{-/-}$ mice vs. controls (Table S1). This phenotype was primarily because of a larger cortical compartment and longer femorae (Fig. 6J and Tables S2 and S3). Bone volume fraction in the femur as measured by microCT in 16-wk $Noc^{-/-}$ mice was significantly greater than controls principally becuase of enhanced trabecular thickness (Fig. 6J and Table S3). Thus, NOC plays an important role in regulating body composition by affecting both hard and soft tissues.

Discussion

The process of adipogenesis includes the differentiation of BMSCs under the influence of adipocyte-specific transcription factors (22, 23). PPAR-γ activation is essential for this process and here we show that NOC enhances PPAR-γ nuclear translocation. Of importance is that although NOC facilitates PPAR-γ nuclear translocation, a PPAR-γ ligand (endogenous or exogenous) is required to activate PPAR-γ transcriptional activity. NOC is a member of a family of proteins that include transcription factors, deadenylases and phosphatases (24). It shares significant sequence similarity to the multifunctional yeast protein Ccr4p, a transcription factor that is involved in regulation of global gene expression in response to nutrient status, in addition to its role as a deadenylase (12, 24, 25). Our initial findings raised the possibility that NOC was functioning at the level of transcription to regulate cell differentiation. However, mammalian NOC lacks the N-terminus activating domain, which Ccr4p possesses (12). In addition, NOC was not detected in the nucleus even with PPAR-γ2 activation, ruling out the possibility that it was a coactivator of PPAR-γ.

Previously PPAR-γ was considered solely in the context of its role as a nuclear receptor and transcription factor, even though cytosolic localization of PPAR-γ has been reported frequently (26–29). However, a nuclear localization signal has never been identified for PPAR-γ, although there is evidence that it is exported from the nucleus in a MEK-dependent manner (30). Thus, the precise mechanism underlying PPAR-γ nuclear translocation remains elusive. Nuclear transport must involve either molecular size-based diffusion or a transport factor acting as a chaperone (31, 32). Our findings raise the intriguing possibility that NOC is involved in the translocation of PPAR-γ, although its absence in the nucleus implies that NOC must function in collaboration with other transport mechanisms to complete the nuclear translocation of PPAR-γ.

In support of that tenet, we found that Noc is induced transiently in early adipogenesis, and then is robustly up-regulated during the latter phases of differentiation in 3T3-L1 cells. The early up-regulation of Noc can be induced by FCS or insulin (15) and may be a critical step in activating PPAR-γ. Indeed, we found that silencing Noc resulted in impaired induction of $Pparg$ transcripts during early adipogenesis in 3T3-L1 cells. Previously, we reported that in U-33 mesenchymal stromal cells transfected with a $Pparg2$ expression construct and treated with rosiglitazone, Noc expression was enhanced nearly 30-fold, implying that Noc was a down-stream target of $Pparg$ (16). In addition, a $Pparg$ "gain-of-function" 6T congenic mouse, which exhibits low bone mass and high marrow adiposity, showed increased Noc expression in fat, liver, and bone marrow (17, 33). Thus, the robust up-regulation of Noc expression in late adipogenesis may be explained in part by increased $Pparg$ expression. In sum, Noc and $Pparg$ may activate each other during adipogenesis, although we cannot rule out the possibility that Noc may also function to deadenylate one of the 3′UTR forms of $Pparg$, thereby acting as negative feedback on nuclear receptor activation.

Further evidence that NOC is important in PPAR-γ regulation comes from our in vivo studies of $Noc^{-/-}$ mice. These mice have

high bone mass and reduced marrow adiposity, a phenotype remarkably similar to that reported in $Pparg^{+/-}$ mice (6). Moreover, the absence of $Pparg$ circadian rhythmicity in the $Noc^{-/-}$ mice, even on a HFD, suggests that NOC modulates PPAR-γ activity in a forward direction.

It is well established that PPAR-γ is an important regulator of mesenchymal stem-cell fate, and its activation favors adipogenesis over osteoblastogenesis partly by suppressing osteogenic signaling pathways, such as Wnt, TGFβ/BMP, IGF-I, and transcription factors, including Runx2 and OSX (osterix) (16, 34–36). Because $Pparg$ expression is lower and $Runx2$ expression is higher in $Noc^{-/-}$ COBs compared with control cells, alterations in cell specification of BMSCs may be responsible for the skeletal phenotype of $Noc^{-/-}$ mice. Similarly, mice with a conditional deletion of circadian genes in osteoblasts, such as $period$ and $cryptochrome$, also exhibit a high bone-mass phenotype (11). Moreover, type I collagen and osteocalcin exhibit significant periodicity during a 24-h cycle, suggesting that bone remodeling is under the control of the circadian clock (37). Because Noc may also be regulated by other clock genes (38, 39) that are important in bone turnover, it is conceivable that Noc modulates skeletal acquisition by functioning as a downstream modulator of osteoblast differentiation.

Adjusting cell behavior to energy availability is a central function of cell physiology (1). Recently, Lamia et al. reported that AMPK, a peripheral sensor of nutrient availability, phosphorylates cryptochrome 1, thereby promoting its ubiquitination and subsequent degradation (40). Previously, we have shown that Noc is rapidly induced in NIH 3T3 cells by FCS (15). In this study, we found that Noc was up-regulated by FCS and insulin in 3T3-L1 preadipocytes (Fig S7). Noc was also up-regulated by FCS in BMSCs, but the induction was not as great as that in 3T3-L1 cells (Fig S7). Insulin did not have any effect on Noc induction in BMSCs. These findings suggest that Noc expression is regulated by external stimuli, although the effect on Noc induction is likely to be cell-specific. The possibility that NOC regulates PPAR-γ nuclear transport provides a unique mechanism whereby fine tuning of adipogenesis can occur in response to entrainment from nutrient excess. The evolution of Noc in the mammalian organism as a nuclear activator for PPAR-γ raises a series of provocative questions about the role energy sufficiency plays in skeletal and adipogenic homeostasis and how environmentally induced alterations could ultimately affect body composition.

Methods

Mice. Generation of $Ccrn4l^{tm1Bjc}$, which we refer to nocturnin knockout mice ($Noc^{-/-}$ mice) has been described previously (19). The original mice were backcrossed onto C57BL/6J background for at least seven generations. All experimental studies were performed using female mice. All of the animal studies were reviewed and approved by the Institutional Animal Care and Use Committee of Maine Medical Center Research Institute.

Cell Culture. See *SI Methods* for details.

Constructs. The pCMV-WT-Noc-Flag, and pCMV-E193A-Noc-Flag vector, which harbors a point mutation in the Mg^{2+} binding motif leading to loss of deadenylase activity, have been previously described (15). Details for other constructs are described in *SI Methods*.

Body Composition and Skeletal Phenotyping of $Noc^{-/-}$ Mice. Whole-body aBMD and aBMC, femoral aBMD and aBMC, and body composition were analyzed using dual-energy x-ray absorptiometry. Peripheral quantitative CT was used to analyze femur length and cortical thickness. Microarchitecture of distal trabecular bone and midshaft cortical bone of femur were evaluated by MicroCT. See *SI Methods* for details.

Analysis for the Role of NOC in Adipogenesis and Osteoblastogenesis. Noc was overexpressed using retrovirus in 3T3-L1 cells and MC3T3-E1 cells to evaluate the role of NOC in adipogenesis and osteoblastogenesis. Noc expression was suppressed using small interfering RNA or short-hairpin RNA in 3T3-L1 cells and

MC3T3-E1 cells. The expression of marker genes and specific staining were used to evaluate adipogenesis and osteoblastogenesis as described in *SI Methods*.

Intracellular Localization of NOC and PPAR-γ2. Intracellular localization of NOC was analyzed by immunofluorescence and Western blot analyses as described in *SI Methods*. A lipophilic tracer [either DiIC$_{18}$(5) (DiD) or DOPE-rhodamine] was used to visualize nuclear membrane. For nuclear staining, cells were stained with either TOPRO3 or SYTOX (Invitrogen).

Analysis of Interaction Between NOC and PPAR-γ2. To analyze the physical interaction between NOC and PPAR-γ2, HEK293 cells were transfected with Pparg2 expression vector and either WT-Noc-Flag or E193A-Noc-Flag expression vector, and immunoprecipitated with anti-Flag antibody. Then, Western blot analysis for PPAR-γ was performed as described in *SI Methods*.

Reporter assay using PPRE-Luc vector was performed in HEK293 cells to analyze the role of NOC in Pparg transcriptional activity as described in *SI Methods*.

Statistical Analysis. All data are expressed as the mean ± SEM. Results were analyzed for statistically significant differences using Student's *t* test or ANOVA followed by Bonferroni multiple comparison post hoc test. The glucose tolerance test was analyzed using repeat measures ANOVA. Statistical significance was set at $P < 0.05$.

1. Gallego M, Virshup DM (2007) Post-translational modifications regulate the ticking of the circadian clock. *Nat Rev Mol Cell Biol* 8:139–148.
2. Balsalobre A, et al. (2000) Resetting of circadian time in peripheral tissues by glucocorticoid signaling. *Science* 289:2344–2347.
3. Zvonic S, Floyd ZE, Mynatt RL, Gimble JM (2007) Circadian rhythms and the regulation of metabolic tissue function and energy homeostasis. *Obesity (Silver Spring)* 15:539–543.
4. Yang X, et al. (2006) Nuclear receptor expression links the circadian clock to metabolism. *Cell* 126:801–810.
5. Lecka-Czernik B, Suva LJ (2006) Resolving the two "bony" faces of PPAR-gamma. *PPAR Res* 2006:27489.
6. Akune T, et al. (2004) PPARgamma insufficiency enhances osteogenesis through osteoblast formation from bone marrow progenitors. *J Clin Invest* 113:846–855.
7. Turek FW, et al. (2005) Obesity and metabolic syndrome in circadian clock mutant mice. *Science* 308:1043–1045.
8. Rudic RD, et al. (2004) BMAL1 and CLOCK, two essential components of the circadian clock, are involved in glucose homeostasis. *PLoS Biol* 2:e377.
9. Oishi K, et al. (2006) Disrupted fat absorption attenuates obesity induced by a high-fat diet in Clock mutant mice. *FEBS Lett* 580:127–130.
10. Shimba S, et al. (2005) Brain and muscle Arnt-like protein-1 (BMAL1), a component of the molecular clock, regulates adipogenesis. *Proc Natl Acad Sci USA* 102:12071–12076.
11. Fu L, Patel MS, Bradley A, Wagner EF, Karsenty G (2005) The molecular clock mediates leptin-regulated bone formation. *Cell* 122:803–815.
12. Green CB, Besharse JC (1996) Identification of a novel vertebrate circadian clock-regulated gene encoding the protein nocturnin. *Proc Natl Acad Sci USA* 93:14884–14888.
13. Wang Y, et al. (2001) Rhythmic expression of Nocturnin mRNA in multiple tissues of the mouse. *BMC Dev Biol* 1:9.
14. Baggs JE, Green CB (2003) Nocturnin, a deadenylase in *Xenopus laevis* retina: A mechanism for posttranscriptional control of circadian-related mRNA. *Curr Biol* 13:189–198.
15. Garbarino-Pico E, et al. (2007) Immediate early response of the circadian polyA ribonuclease nocturnin to two extracellular stimuli. *RNA* 13:745–755.
16. Shockley KR, et al. (2009) PPARgamma2 nuclear receptor controls multiple regulatory pathways of osteoblast differentiation from marrow mesenchymal stem cells. *J Cell Biochem* 106:232–246.
17. Kawai M, et al. (2010) Nocturnin: A circadian target of Pparg-induced adipogenesis. *Ann N Y Acad Sci* 1192:131–138.
18. Cao SX, Dhahbi JM, Mote PL, Spindler SR (2001) Genomic profiling of short- and long-term caloric restriction effects in the liver of aging mice. *Proc Natl Acad Sci USA* 98:10630–10635.
19. Green CB, et al. (2007) Loss of Nocturnin, a circadian deadenylase, confers resistance to hepatic steatosis and diet-induced obesity. *Proc Natl Acad Sci USA* 104:9888–9893.
20. Ho A, Schwarze SR, Mermelstein SJ, Waksman G, Dowdy SF (2001) Synthetic protein transduction domains: enhanced transduction potential in vitro and in vivo. *Cancer Res* 61:474–477.
21. Cooper MP, Uldry M, Kajimura S, Arany Z, Spiegelman BM (2008) Modulation of PGC-1 coactivator pathways in brown fat differentiation through LRP130. *J Biol Chem* 283:31960–31967.
22. Tontonoz P, Spiegelman BM (2008) Fat and beyond: The diverse biology of PPARgamma. *Annu Rev Biochem* 77:289–312.
23. Rosen ED, MacDougald OA (2006) Adipocyte differentiation from the inside out. *Nat Rev Mol Cell Biol* 7:885–896.
24. Dupressoir A, et al. (2001) Identification of four families of yCCR4- and Mg2+-dependent endonuclease-related proteins in higher eukaryotes, and characterization of orthologs of yCCR4 with a conserved leucine-rich repeat essential for hCAF1/hPOP2 binding. *BMC Genomics* 2:9.
25. Tucker M, et al. (2001) The transcription factor associated Ccr4 and Caf1 proteins are components of the major cytoplasmic mRNA deadenylase in *Saccharomyces cerevisiae*. *Cell* 104:377–386.
26. Burgermeister E, Seger R (2007) MAPK kinases as nucleo-cytoplasmic shuttles for PPARgamma. *Cell Cycle* 6:1539–1548.
27. Thuillier P, Baillie R, Sha X, Clarke SD (1998) Cytosolic and nuclear distribution of PPARgamma2 in differentiating 3T3-L1 preadipocytes. *J Lipid Res* 39:2329–2338.
28. Shibuya A, et al. (2002) Nitration of PPARgamma inhibits ligand-dependent translocation into the nucleus in a macrophage-like cell line, RAW 264. *FEBS Lett* 525:43–47.
29. Kelly D, et al. (2004) Commensal anaerobic gut bacteria attenuate inflammation by regulating nuclear-cytoplasmic shuttling of PPAR-gamma and RelA. *Nat Immunol* 5:104–112.
30. Burgermeister E, et al. (2007) Interaction with MEK causes nuclear export and downregulation of peroxisome proliferator-activated receptor gamma. *Mol Cell Biol* 27:803–817.
31. Lusk CP, Blobel G, King MC (2007) Highway to the inner nuclear membrane: Rules for the road. *Nat Rev Mol Cell Biol* 8:414–420.
32. Stewart M (2007) Molecular mechanism of the nuclear protein import cycle. *Nat Rev Mol Cell Biol* 8:195–208.
33. Rosen CJ, et al. (2004) Congenic mice with low serum IGF-I have increased body fat, reduced bone mineral density, and an altered osteoblast differentiation program. *Bone* 35:1046–1058.
34. Ali AA, et al. (2005) Rosiglitazone causes bone loss in mice by suppressing osteoblast differentiation and bone formation. *Endocrinology* 146:1226–1235.
35. Rzonca SO, Suva LJ, Gaddy D, Montague DC, Lecka-Czernik B (2004) Bone is a target for the antidiabetic compound rosiglitazone. *Endocrinology* 145:401–406.
36. Kawai M, Sousa KM, MacDougald OA, Rosen CJ (2010) The many facets of PPAR {gamma}: Novel insights for the skeleton. *Am J Physiol Endocrinol Metab*, 10.1152/ajpendo.00157.2010.
37. Gundberg CM, Markowitz ME, Mizruchi M, Rosen JF (1985) Osteocalcin in human serum: A circadian rhythm. *J Clin Endocrinol Metab* 60:736–739.
38. Li R, et al. (2008) CLOCK/BMAL1 regulates human nocturnin transcription through binding to the E-box of nocturnin promoter. *Mol Cell Biochem* 317:169–177.
39. Oishi K, et al. (2003) Genome-wide expression analysis of mouse liver reveals CLOCK-regulated circadian output genes. *J Biol Chem* 278:41519–41527.
40. Lamia KA, et al. (2009) AMPK regulates the circadian clock by cryptochrome phosphorylation and degradation. *Science* 326:437–440.

CELL BIOLOGY